

Strategy to Produce High-Void Fraction in Microcellular Foamed Polyolefins

Pornchai Rachtanapun^{1*}, and Susan E. M. Selke²

¹ *Department of Packaging Technology, Faculty of Agro-Industry, Chiang Mai University, Chiang Mai 50200, Thailand*

² *School of Packaging, Michigan State University, East Lansing, Michigan 48824, USA*

*Corresponding author. E-mail: p.rachta@chiangmai.ac.th

ABSTRACT

In this research, a strategy to achieve high-void fractions in microcellular foamed polyolefins was investigated. The effects of batch processing conditions (time and temperature) and blend composition on the void fraction of microcellular foamed HDPE, PP and HDPE/PP blends were studied. Blending decreased the crystallinity of HDPE and PP in the HDPE/PP blends and facilitated microcellular foam production in blend materials. The void fraction of the foamed polymer blends was strongly dependent on the processing conditions: time (5, 10, 20 and 30 sec) and temperature (135, 160 and 175°C), and on blend composition. To achieve a high-void fraction, a foaming time of at least 20 seconds and a foaming temperature significantly above melting temperature were required. The blend ratio also affected the ability to achieve a high-void fraction.

Key words: Microcellular foams, Polyolefin, Polymer blends

INTRODUCTION

Microcellular plastics are characterized by cell densities in the range of 10⁹ to 10¹⁵ cells per cubic centimeter, and cell sizes in the range of 0.1 to 10 micrometers. There are three major steps in producing microcellular foams, utilizing thermodynamic instability of a gas polymer system (Martini et al., 1984): 1) polymer/gas solution formation by saturating a polymer with a high-pressure gas, 2) microcellular nucleation and 3) cell growth and density reduction. In general, achieving a foam structure in a semi-crystalline polymer is relatively difficult compared to an amorphous polymer (Doroudiani et al., 1998). In this study, the effect of processing conditions (foaming time and foaming temperature) and blend composition on the void fraction in microcellular foaming of neat HDPE, PP and HDPE/PP blends was investigated. First, a variety of blend compositions were prepared using a twin-screw extruder. These materials were compression-molded into panels in a hot hydraulic press. Samples with differing blend compositions were then foamed, varying the foaming time and temperature and their void fractions compared.

Over the past decade, interest in the production of microcellular plastics has grown for several reasons. Compared to conventional foams in which weight reduction leads to reduction in mechanical properties, these materials exhibit enhanced impact strength (Dor-

oudiani et al., 1998; Matuana et al., 1998a, 1998b), toughness (Baldwin et al., 1992; Collias et al., 1994; Matuana et al., 1998b), fatigue life (Seeler and Kumar, 1993, 1994) and thermal stability (Shimbo et al., 1992). They offer a reduction in material usage at the same time. The specific density reduction of these materials can reach 75% or higher (Kumar and Suh, 1988). With such unique properties, there are a large number of innovative potential applications for microcellular foam plastics. These include packaging with reduced material costs, airplane and automotive parts with high strength-to-weight ratios and sports equipment with reduced weight and high energy absorption.

Over the last decade, the research on microcellular foams has mainly focused on the foaming of amorphous polymers, for example, polystyrene (Kweeder et al., 1991), poly(vinylchloride) (Kumar and Suh, 1988), polycarbonate (Kumar and Vander Wel, 1991; Kumar and Weller, 1991; Shimbo et al., 1992) and poly(methyl methacrylate) (Geol and Beckman, 1994). Only limited research has been done on the foaming of semicrystalline polymers. Microcellular foamed semicrystalline polymers are difficult to achieve because of high crystallinity and size of crystallites (Doroudiani et al., 1996, 1998). Cell structures usually developed only on the surface of the polymer samples (Doroudiani et al., 1998). Colton (1989) described three major problems: low gas solubility in the crystalline region, the requirement to foam near the melting temperature and the physical size and structure of the crystallites. He studied microcellular foams of PP and found that microcellular foam PP was produced successfully by adding appropriate nucleating agents. Microcellular foams of ethylene-propylene copolymers could be produced without the nucleating agent at temperatures above the melting temperature because of the lower surface tension in the copolymer. Doroudiani et al., (1996) reported that the morphology of semicrystalline polymers had a great influence on the solubility and diffusivity of the blowing agent and on the cellular structure of the microcellular foam produced in a batch process. Microcellular foams of high-density polyethylene (HDPE) and polypropylene (PP) were difficult to achieve by batch foam processing except by quenching the polymer during cooling from the melt to achieve a relative low crystallinity (Doroudiani et al., 1996). In recent research, microcellular foams were greatly enhanced by using HDPE/isotactic PP blends (Doroudiani et al., 1998). The experiment was carried out on five ratios of blend composition of HDPE/isotactic PP: 0/100, 10/90, 50/50, 90/10 and 100/0. Doroudiani et al. reported that the blending decreased the crystallinity of iPP in the blends and the presence of another phase had a large effect on the crystalline morphology in all the blends. The blend with 50/50 HDPE/iPP gave a non-uniform structure and had a very high volume expansion ratio but the other four compositions gave low volume expansion ratios (Doroudiani et al., 1998).

Problem Statement

The feasibility of developing a microcellular structure in HDPE/iPP blends has been successfully demonstrated (Doroudiani et al., 1998). However, only one blend composition resulted in a high volume expansion ratio and the foam was non-uniform. Therefore, the purpose of this study was to identify a strategy that can achieve a high-void fraction in polyolefins.

The objectives of the study were to investigate the effects of the processing conditions (foaming time and temperature) and blend composition on the void fraction. The effects of blend composition and crystallinity on solubility and diffusion of CO₂ and consequently on the void fraction were also investigated.

EXPERIMENTATION

Materials

Injection-molding-grade HDPE (Dow HDPE 00452N, melt index 4g/10 min (ASTM D1238), density 0.952 g/cc) and extrusion-and injection-molding-grade polypropylene homopolymer (PP) (INSPIRE H704-04, melt flow rate 4 g/10 min (ASTM D1238), density 0.90 g/cc) were used. Commercial-grade carbon dioxide was used as a blowing agent. All chemicals were used as received from the manufacturers.

Manufacture of the Polyolefin and Blend Samples

In this study, the effects of blend composition, time and temperature on void fraction were investigated. Samples of HDPE, PP and their blends with compositions of 100:0, 70:30, 50:50, 30:70 and 0:100, respectively, were manufactured using a Baker Perkins Model ZSK-30, 30 mm, 26:1 co-rotating twin-screw extruder (Werner & Pfleiderer Corporation, Ramsey, New Jersey). The extruder provided six temperature control points (heaters), and two different temperature profiles were used. For HDPE, temperatures were set at 155°C for all six zones. For PP and blends, temperatures were set at 180°C in the first 2 zones and 155°C in the remaining 4.

The screw speed was set at 100 rpm. The extruded mixture was cut into six-inch length before it solidified at room temperature.

The extruded samples were compression-molded into panels (2 mm in thickness) in a hydraulic press at 160°C for HDPE and 185°C for PP and blends for 5 minutes, using 30,000 psi. From these panels, 1/2 inch by 1 inch rectangular test specimens were cut (using a New Hermes Safety Saw).

Sorption Experiments

The diffusion and saturated concentration of gas (solubility of gas) in the samples were measured in the sorption experiment. The samples were saturated in a pressure vessel with carbon dioxide at room temperature (23–25°C) and 5.51 MPa (800 psi) for 24 hours. This length of time was determined to be sufficient for saturation, based on work by Doroudiani et al. (1998). CO₂ uptake (solubility) was measured by weight gain immediately after pressure release, using a digital balance readable to 0.0001 g (Mettler model AB 204) (Matuana et al., 1996, 1997; Matuana and Mengeloglu, 2001). Solubility of CO₂ can be predicted by the rule of mixtures using (Doroudiani et al., 1998):

$$k_b = k_{HDPE} (Portion_{HDPE}) + k_{PP} (Portion_{PP}) \quad (1)$$

where k_b , k_{HDPE} and k_{PP} are the solubility of CO₂ in the blends, HDPE region and PP region, respectively. The crystalline regions have very tight packing of polymer chains in which gas solubility is negligible (Colton, 1989; Doroudiani et al., 1996, 1998). Therefore, the solubility of CO₂ in the blends can also be calculated by (Doroudiani et al., 1998):

$$k_b = k_{am,HDPE} (1 - \chi_{HDPE}) (Portion_{HDPE}) + k_{am,PP} (1 - \chi_{PP}) (Portion_{PP}) \quad (2)$$

where $k_{am,HDPE}$ and $k_{am,PP}$ are the solubilities of CO₂ in the amorphous regions of HDPE and PP, respectively, and χ_{HDPE} and χ_{PP} are the crystalline fractions of HDPE and of PP in

the blends, respectively. The solubilities of CO₂ in the amorphous regions can also be calculated from the measured solubilities of CO₂ in pure HDPE and PP from the sorption experiments, and the crystallinities of pure HDPE and PP from DSC experiments, using the following equations (Doroudiani et al., 1998):

$$K_{measuredHDPE} = K_{amorphousHDPE}(1 - \chi_{HDPE}) \quad (3)$$

$$K_{measuredPP} = K_{amorphousPP}(1 - \chi_{PP}) \quad (4)$$

The crystallinities of the HDPE and PP are 73.27% and 49.17%, respectively (Table 1). The measured solubilities of CO₂ in the pure HDPE and PP are 2.136 and 4.22, respectively (Table 2). The calculated $K_{amorphousHDPE}$ and $K_{amorphousPP}$ are 7.99 and 8.30 wt%, respectively, and these values were substituted in Equation 2. Therefore, the solubility of CO₂ in the blends can be calculated by (Doroudiani et al., 1998):

$$K_b = 7.99(1 - \chi_{HDPE})(Portion_{HDPE}) + 8.30(1 - \chi_{PP})(Portion_{PP}) \quad (5)$$

Weight loss as a function of $t^{1/2}/l$ was used to determine the diffusion coefficient (Matuana et al., 1996, 1997; Matuana and Mengeloglu, 2001). The diffusivity of gas (D) was determined, using the following equation (Matuana and Mengeloglu, 2001):

$$D = \frac{\pi}{16} \left[\frac{d\left(\frac{M_t}{M_\infty}\right)}{d\left(\frac{t}{l}\right)} \right]^2 \quad (6)$$

where M_t is the total amount of gas loss at time (t) from the polymer matrix, M_∞ is the total amount of gas uptake at infinite time and l is the thickness of the sample (Matuana and Mengeloglu, 2001).

Microcellular Foaming Experiments

Batch microcellular foaming experiments were conducted as follow. The saturated samples were foamed via a rapid solubility drop through a pressure decrease and a temperature increase. These saturated samples were taken out of the pressure vessel and then immediately immersed in a hot glycerin bath at three foaming temperatures (135°C, 160°C and 175°C) for four foaming times of 5s, 10s, 20s and 30s. After the specified foaming time, samples were immediately quenched in cold water (Matuana et al., 1996, 1997; Matuana and Mengeloglu, 2001).

Characterization of Foams

The weights of unfoamed and foamed samples were measured in air (Ma) and in distilled water (Mw) to determine the respective densities ρ and ρ_f (g/cc). All measurements were made according to ASTM standard D-792. At least five specimens for each sample were

tested, and the reported density is the average of these measurements. The density of the material was determined by (Matuana et al., 1996, 1997; Matuana and Mengeloglu, 2001):

$$Density = 0.9975 \left(\frac{M_a}{M_w} \right) \quad (7)$$

the void fraction (V_f) was calculated by the following equation (Matuana et al., 1996, 1997; Matuana and Mengeloglu, 2001):

$$V_f = 1 - \frac{\rho_f}{\rho} \quad (8)$$

Differential Scanning Calorimetry (DSC)

DSC was performed, using a DSC 2010 (TA Instruments) to investigate the crystallinities of the HDPE, PP and their blends. The calibration for heat capacity was performed by running an indium reference standard. Three to five replicates were heated from room temperature to 200°C, using a heating rate of 10°C/min. Nitrogen was used as a purge gas with a flow rate of 50 ml/minute. Sample weights of 3–5 mg were used. The crystallinities of HDPE and PP were calculated as follow: For the pure polymer

$$\chi_{HDPE}(\%) = \frac{\Delta H_{m,HDPE}}{\Delta H_{m,HDPE}^{\circ}} \times 100\% \quad (9)$$

$$\chi_{PP}(\%) = \frac{\Delta H_{m,PP}}{\Delta H_{m,PP}^{\circ}} \times 100\% \quad (10)$$

For each component in the blend

$$\chi_{HDPE}(\%) = \frac{\Delta H_{m,HDPE}}{\Delta H_{m,HDPE(1-x)}^{\circ}} \times 100\% \quad (11)$$

$$\chi_{PP}(\%) = \frac{\Delta H_{m,PP}}{\Delta H_{m,PP(x)}^{\circ}} \times 100\% \quad (12)$$

For the total sample:

$$\chi_{total} = (\%HDPE)(\% \chi_{HDPE}) + (\%PP)(\chi_{PP}) \quad (13)$$

where χ_{HDPE} and χ_{PP} are percent crystallinity in HDPE and PP, respectively. Heats of fusion for HDPE ($\Delta H_{m,HDPE}^{\circ}$) and PP ($\Delta H_{m,PP}^{\circ}$) are 293 J/g and 209 J/g (Wunderlich, 1973; Doroudiani et al., 1998). Heats required for melting the HDPE phase ($\Delta H_{m,HDPE}$) and PP phase ($\Delta H_{m,PP}$) were measured by DSC (J/g), and x is the weight fraction of PP in the blend.

Statistical Analysis

Data were analyzed by ANOVA and Tukey's Studentized Range (HSD) test, using the SAS software program ($\alpha = 0.05$).

RESULTS AND DISCUSSION

Effects of Polymer Blend Composition on Solubility and Diffusivity of Carbon Dioxide

It is known that the foamability of polymers is affected by the sorption of gas in the polymer, and that the mechanisms of cell nucleation and cell growth are influenced by the amount of the gas dissolved in the polymer and the rate of gas diffusion (Shimbo et al., 1992; Matuana et al., 1996, 1997; Doroudiani et al., 1998; Matuana and Mengelglu, 2001). As shown in Figure 1, the amount of CO₂ gas dissolved (measured solubility) decreased as the ratio of HDPE increased. The measured solubility of gas was strongly dependent on the total crystallinity of the polymer (Table 1). When the HDPE component increased, the total crystallinity increased and the solubility of gas decreased, as CO₂ gas dissolves only in the amorphous regions (Colton 1989; Doroudiani et al. 1996, 1998; Matuana et al., 1996, 1997; Matuana and Mengelglu, 2001) (Figure 1).

Table 1. Melting Temperature (T_m) and Percent Crystallinity (χ) of Blend Samples.

Blends	$T_{m,HDPE}(^{\circ}C)$	$\chi_{HDPE}(\%)$	$T_{m,PP}(^{\circ}C)$	$\chi_{PP}(\%)$	Total % χ in Blends
HDPE	132.09	73.27	-	-	73.27
70:30	130.01	68.63	163.42	43.36	61.05
50:50	129.96	63.46	162.36	40.12	51.79
30:70	128.75	61.89	163.78	43.78	49.21
PP	-	-	164.23	49.17	49.17

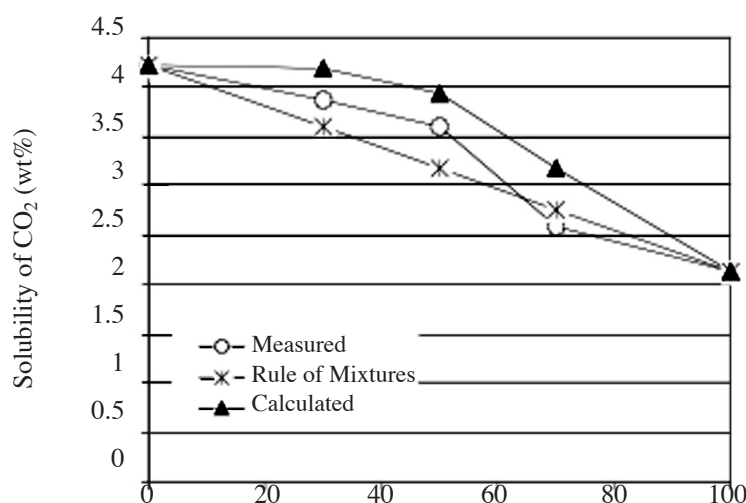


Figure 1. Effects of blend composition on solubility of CO₂ in polyolefin blends.

The amount of crystallinity in blends was less than that in the pure polymers. Therefore, the predicted solubilities based on the rule of mixtures (Equation 1) were less than the experimental results because of using the crystallinity of the pure polymer in the calculation. The calculated solubilities based on Equation 3, using crystallinity measured in DSC experiments, were slightly higher than the experimental results (Figure 1 and Table 2). These results are in agreement with Doroudiani et al., (1998).

Table 2. The Measured Solubility of CO₂ content in Neat Polymers and Blends as a Function of Blend Composition.

Blend Compositon, %HDPE	Measured Solubility of CO ₂ Content (wt%)		
	Measured	Rule of mixtures	Calculated from DSC
100	2.14	2.14	2.14
70	2.58	2.76	3.17
50	3.59	3.18	3.93
30	3.86	3.59	4.18
0	4.22	4.22	4.22

The desorption curve of CO₂ in the polyolefin blends is shown in Figure 2. The diffusivity of CO₂ was calculated from the desorption curve. The desorption curve for CO₂ is relatively, not strongly, influenced by blend composition. At $M_t/M_\infty = 0.5$, Equation 4 gives (Matuana and Mengelglu, 2001):

$$D = \frac{0.049}{(t/l)} \tag{14}$$

The calculated diffusivity of CO₂ in the blends (D) is shown in Figure 3. The diffusivity of CO₂ decreased as the HDPE component increased. As expected, as the total amount of crystallinity increased, the diffusivity of CO₂ decreased. The change in diffusivity was most dramatic from pure PP to the 50:50 HDPE/PP blend, with only a slight decrease as the proportion of HDPE increased to 100%.

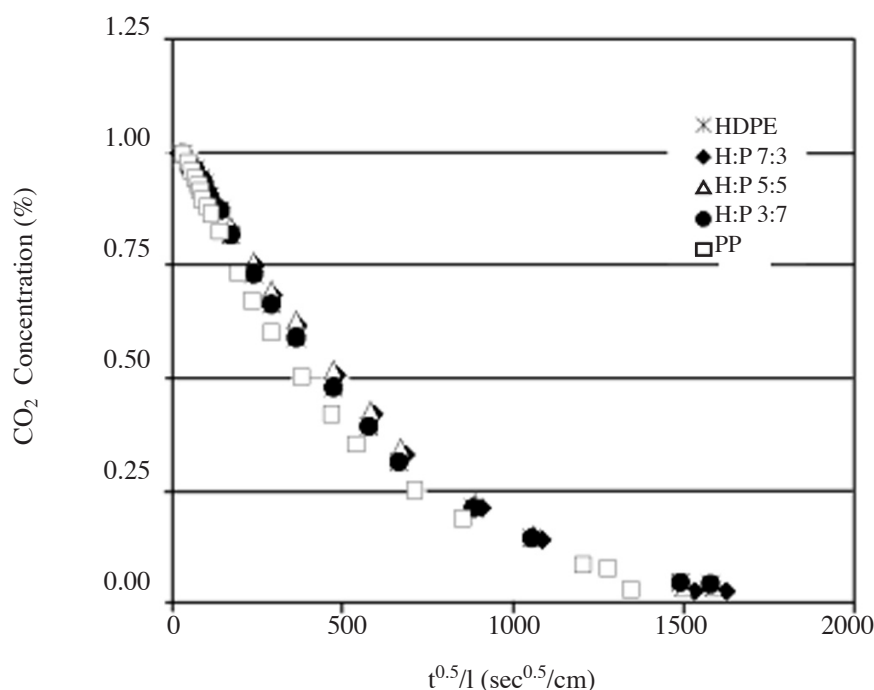


Figure 2. Desorption curve of CO₂ in polymer blends.

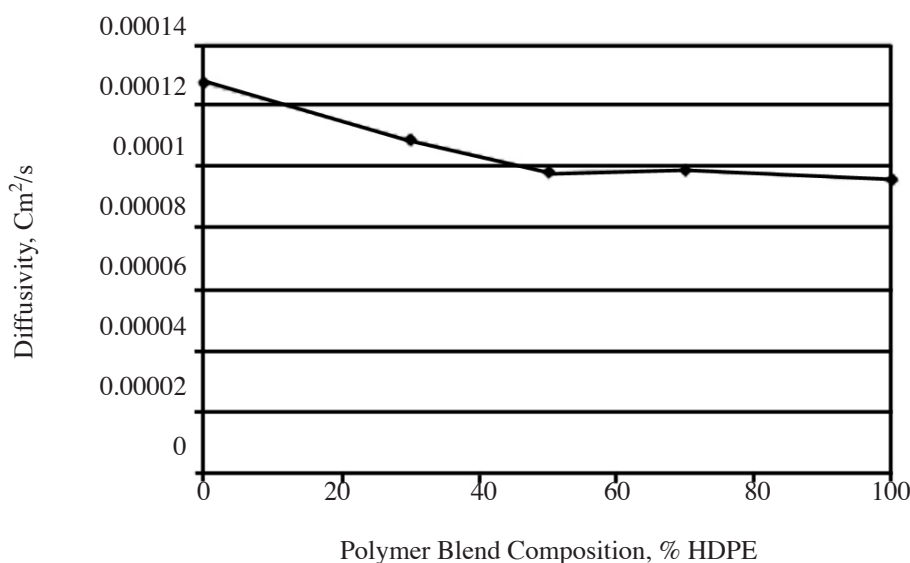


Figure 3. Effect of blend composition on diffusivity of CO₂.

Differential Scanning Calorimetry

The crystallinity of the neat polymers and each component in the blends as well as the total amount of crystallinity in the samples were measured in the DSC experiments. The crystalline fraction of HDPE dramatically decreased as the PP component increased, while the crystalline fraction of PP decreased only slightly as the HDPE component increased, as shown in Table 1. The melting temperature results confirmed this finding. The melting tem-

perature of HDPE decreased as the amount of the PP increased. For example, the HDPE melting temperature decreased from 132.09°C to 130.01, 129.96, and 128.75°C as the PP component increased to 30, 50, and 70%, respectively. The melting temperature of PP decreased only slightly. As shown in Table 1, the total amount of crystallinity of the blends decreased as the PP component increased because the crystalline fraction of HDPE was reduced by the PP component. In contrast, Martuscelli (1984) and Doroudiani et al., (1998) found that the presence of HDPE melt retarded the crystallization of PP more than the reverse. This behavior should be investigated further.

Effects of Foaming Time and Temperature on Void Fraction

The effects of foaming time and temperature on void fraction for HDPE, PP and their blends (HDPE/PP 70:30, 50:50 and 30:70) were investigated. The samples were foamed at various foaming times (5, 10, 20 and 30 sec) and temperatures (135, 160 and 175°C). All results represent the average of five specimens; standard deviations are shown as bars on the graphs.

The effects of foaming time and temperature on void fraction for HDPE are illustrated in Figure 4. When the foaming temperature was low (135°C, slightly above the melting temperature of HDPE), the void fraction was very low. The void fraction tended to slightly increase with longer foaming time, but the increase was not statistically significant. In contrast, the void fraction of the foamed HDPE was strongly dependent on both the foaming time and temperature when the foaming temperature was well above the melting temperature (T_m) of HDPE. The void fraction dramatically increased as foaming time increased. At a foaming temperature of 160°C, the foaming time and void fraction were linearly related. At a foaming temperature of 175°C, the void fraction increased initially with foaming time and leveled off after 20 to 30 seconds.

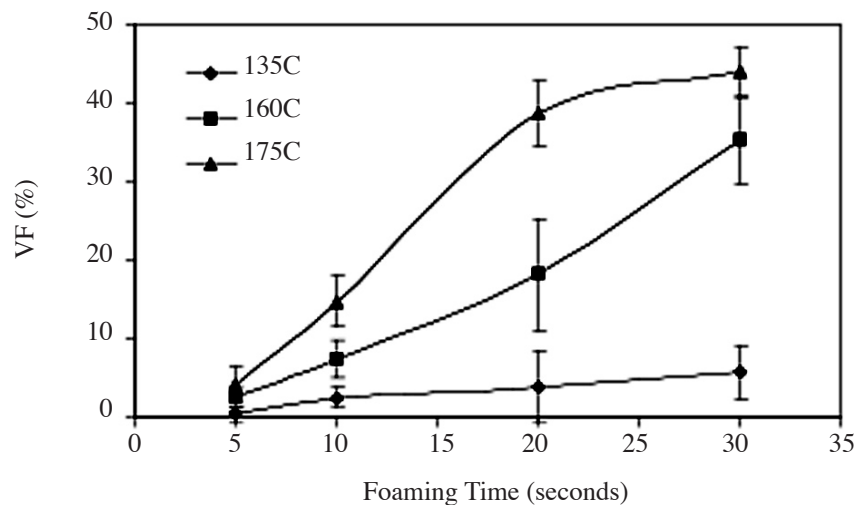


Figure 4. Dependence of void fraction on the foaming time and temperature for HDPE.

Microcellular foamed PP showed similar behavior to HDPE. The void fraction of foamed PP did not significantly increase with foaming time for temperatures below the melting temperature of PP (135 and 160°C) (Figure 5). However, the effect of foaming time on

the void fraction of the microcellular foamed PP was significant at the foaming temperature above the T_m of PP (175°C). When the foaming temperature was well above the T_m of the polymer, the void fraction dramatically increased with foaming time.

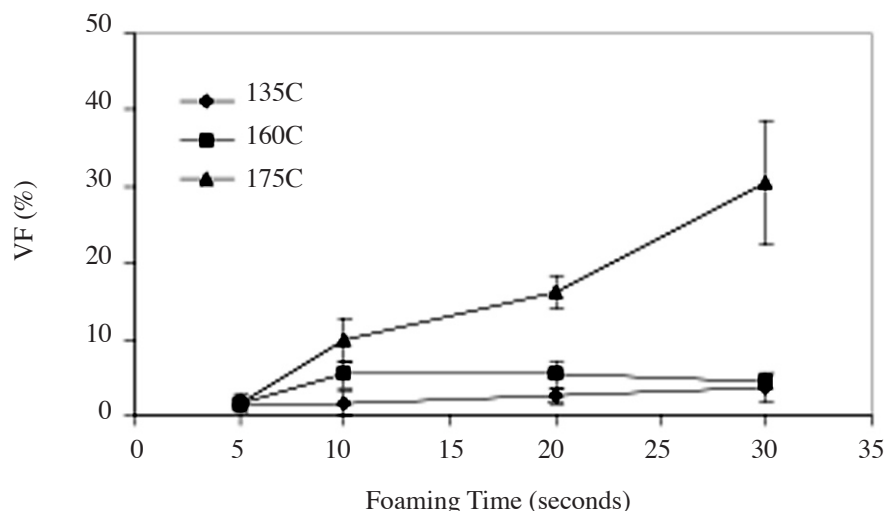


Figure 5. Dependence of void fraction on the foaming time and temperature for PP.

The mechanism of cell growth is controlled by the stiffness of the gas/polymer matrix, the rate of gas diffusion and the amount of gas loss at each foaming time and temperature (Matuana et al., 1997). Typically, an amorphous polymer/gas solution will be heated above its glass transition temperature. The bubbles will start growing and the cell growth will continue until all the dissolved gas has diffused into the cell and then the diffused gases in the cell tend to diffuse out of the cell to the environmental air. Thus, the volume expansion ratio will increase as the gas diffuses from the polymer melt into the cells, and then it tends to level off when the gas is completely depleted from the polymer melt, and finally the volume expansion ratio tends to decline as the gas diffuses into the environmental air (Matuana et al., 1997). However, semi-crystalline polymers are relatively difficult to process into microcellular foams compared to amorphous polymers. Colton (1989) identified three basic problems: the low gas solubility in the crystalline regions, the requirement to foam near the melting temperature and the physical size and structure of the crystals.

The crystallites in the polymer cause very high stiffness and high melt viscosity which prevent bubble growth. The polymer will not flow easily to allow cells to nucleate and grow. Moreover, the driving force of the gas is not high enough to overcome the crystalline attractive forces and entanglements of the polymer (Colton, 1989). In this study, even when the foaming temperature of HDPE was above its T_m at 135°C (3 degrees above the melting temperature of HDPE) and foaming time was long, the void fraction did not significantly increase. This very low generation of foam may be because HDPE is highly-crystalline (above 70%). Therefore, the temperature only 3 degrees above its melting temperature was not high enough to provide adequate energy to disrupt sufficient crystallinity in the polymer to allow the gas to overcome the attractive forces and entanglements and move the polymer chains. Moreover, the high crystallinity results in very tight packing of the polymer chains which leaves little room for the CO_2 gas. Thus, a high concentration of CO_2 gas in HDPE will not

be achieved. The low concentration of gas did not prevent the foaming but produced widely-scattered cells (Colton, 1989). Therefore, HDPE has to be heated high enough above its melt temperature to overcome this problem.

When the foaming temperature was above the melting temperature of HDPE and high enough, the void fraction was dependent on the foaming time. The melt viscosity and the stiffness of the HDPE matrix decreased with long foaming time, perhaps due to the decreasing amount of crystallinity. Moreover, the longer foaming time allowed the molecules more time to move, and this may also be responsible for increasing the void fraction (Matuana et al., 1996, 1997; Matuana and Mengeloglu, 2001). The foaming time at 5 and 10 seconds was too short to achieve a high-void fraction even when the foaming temperature was high.

We can conclude that if we want to achieve a high-void fraction for HDPE, we have to foam sufficiently high above the melting temperature of HDPE, and foam for at least 20 seconds. However, it should be noted that even though we can achieve a high-void fraction, if the foaming temperature is too high and the foaming time is too long, this may cause deformation of the polymer (Matuana et al., 1997). At temperatures above the melting point, the crystallites dissolve and the strength rapidly approaches zero (Colton, 1989). Therefore, the use of too high foaming temperature and too long foaming time may not be desirable for achieving a high-void fraction in a batch process because of the deformation of the polymer matrix, even though the softened polymer matrix is favorable to bubble growth (Matuana et al., 1997).

As shown in Figure 5, the same explanation applies to the behavior of PP. Again, to achieve a high-void fraction required a temperature well above T_m and sufficiently-long foaming time.

The effects of foaming time and temperature on the void fraction of blends of HDPE and PP were also investigated. Figures 6, 7 and 8 show that the void fraction of all the blends (HDPE/PP ratios of 70:30, 50:50 and 30:70) were not significantly different at the low foaming temperature of 135°C for the foaming times investigated. Blending is known to decrease the amount of crystallinity in the blends (Martuscelli, 1984; Doroudiani et al., 1998). In this study, the amount of crystallinity in both the HDPE and PP fractions decreased in the blends. The effect on the degree of the crystallinity was dependent on the ratios of the polymers. However, the foaming temperature of 135°C might be still too low. The polymer matrix remained too stiff and viscous to allow the polymer to move sufficiently to allow significant cell growth.

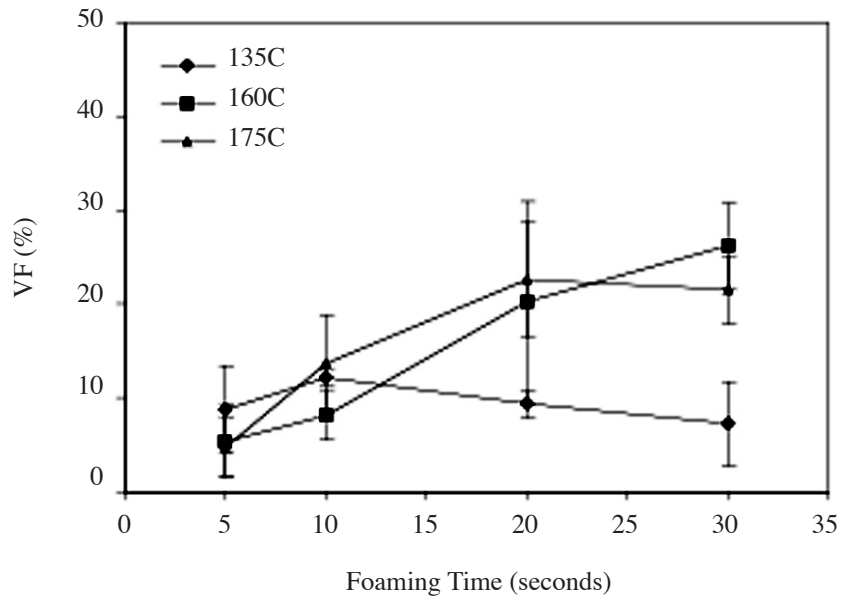


Figure 6. Dependence of void fraction of the foaming time and temperature for 70:30 HDPE/PP.

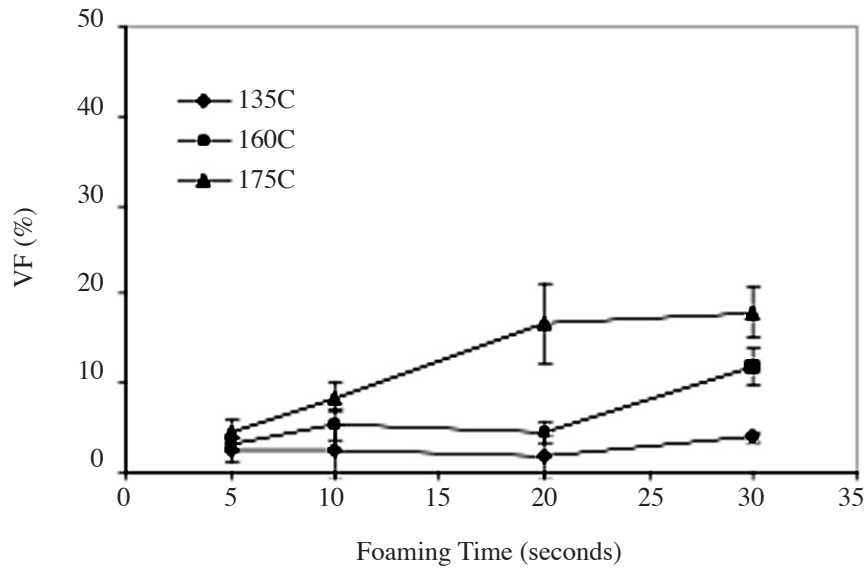


Figure 7. Dependence of void fraction on the foaming time and temperature for 50:50 HDPE/PP.

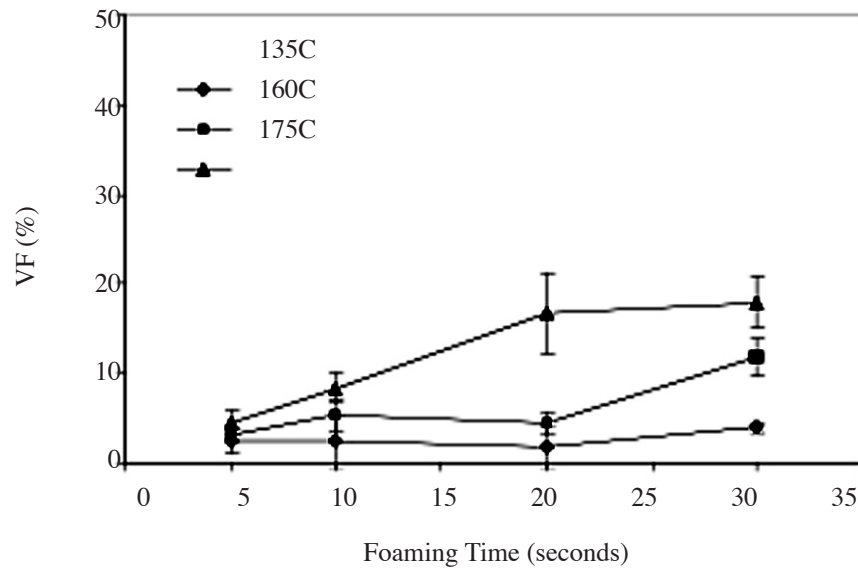


Figure 8. Dependence of void fraction on the foaming time and temperature for 30:70 HDPE/PP.

At higher foaming temperatures (160 and 175°C), the void fraction of foamed 70:30 HDPE/PP increased with foaming time (Figure 6). The trend in this blend was similar to HDPE. At 160°C there was a linear relationship between foaming time and void fraction. At 175°C, the void fraction increased initially with the foaming time and leveled off between 20 and 30 seconds. As discussed for HDPE, the reduced melt viscosity and lowered stiffness of the samples due to the high foaming temperature and long-enough foaming time may be responsible for the increase in the void fraction. Therefore, a high-void fraction could be achieved at high foaming temperatures and a foaming time of at least 20 seconds.

The void fraction of 50:50 HDPE/PP did not increase significantly at foaming times of 5 to 20 seconds at 160°C (Figure 7) but did increase after 30 seconds. The increased ratio of PP in the blend caused the matrix to be much stiffer, as 160°C was below the T_m of PP. However, if the foaming time was long enough, some parts of the polymer chain could move. Also, perhaps the lower activation energy for bubble nucleation between the interfaces of the polymers facilitated gas diffusion into the nucleation sites (Doroudiani et al., 1998). However, the void fraction remained low at this temperature. At a foaming temperature of 175°C, the void fraction increased with the foaming time until 20 seconds and then leveled off. However, the void fraction remained low (below 20%). A high-void fraction was not achieved for this blend ratio.

For 30:70 HDPE/PP blends, at 160°C the void fraction increased with foaming time from 5 to 10 seconds and then leveled off (Figure 8). This behavior was similar to microcellular foamed PP at the same temperature, but the blend was a little higher in void fraction compared to PP, probably because the loss of crystallinity in the HDPE portion made the polymer matrix softer than pure PP, so the polymer chains had more mobility and the bubbles could start nucleating. Moreover, the blend has heterogeneous interfaces, facilitating bubble nucleation. However, the void fraction was still low. Even though the cells were able to nucleate, the polymer matrix was too stiff to allow much cell growth even with long foaming times. Therefore, to achieve a high-void fraction, the foaming temperature should be higher than

the melting temperature of PP. When the foaming temperature was above the melting temperature of PP, the void fraction dramatically increased at long foaming times. The void fraction showed a strong linear dependence on the foaming time.

From this study, we can conclude that the foaming temperature of 135°C and the foaming times of 5 and 10 seconds are not suitable for foaming these polyolefins. The foaming temperature should be significantly higher than the melting temperature of the pure polymer to achieve a high-void fraction for the pure polymer. To achieve a high-void fraction in the blends, the required foaming temperature is dependent on the composition of the blends, for example, 30:70 HDPE/PP should be foamed above the melting point of PP. A high-void fraction was not achieved for 50:50 HDPE/PP.

Effects of Blend Composition on Void Fraction

The effects of blend composition on the void fraction are illustrated in Figures 9, 10 and 11 for foaming temperatures of 135, 160 and 175°C. At the lowest foaming temperature (135°C), the blend compositions of 70:30 and 30:70 HDPE/PP tended to give slightly higher void fractions, but the differences were not statistically significant. At the 160°C foaming temperature, only pure HDPE and 70:30 HDPE/PP at 20–30 seconds foaming time achieved a high-void fraction. At 175°C foaming temperature, Figure 8 shows the strong dependence of void fraction on the blend composition and foaming time. To achieve a high-void fraction for blends, the foaming time has to be longer than 20 seconds.

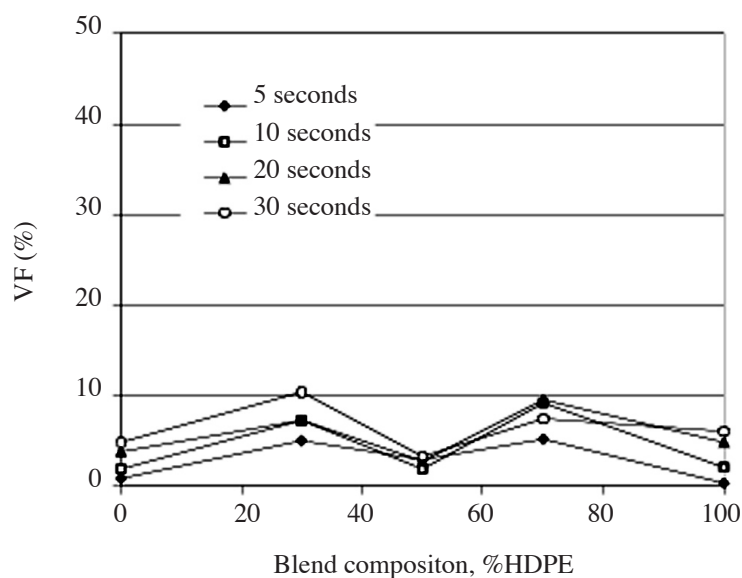


Figure 9. Effect of foaming time and blend composition on the void fraction at 135°C.

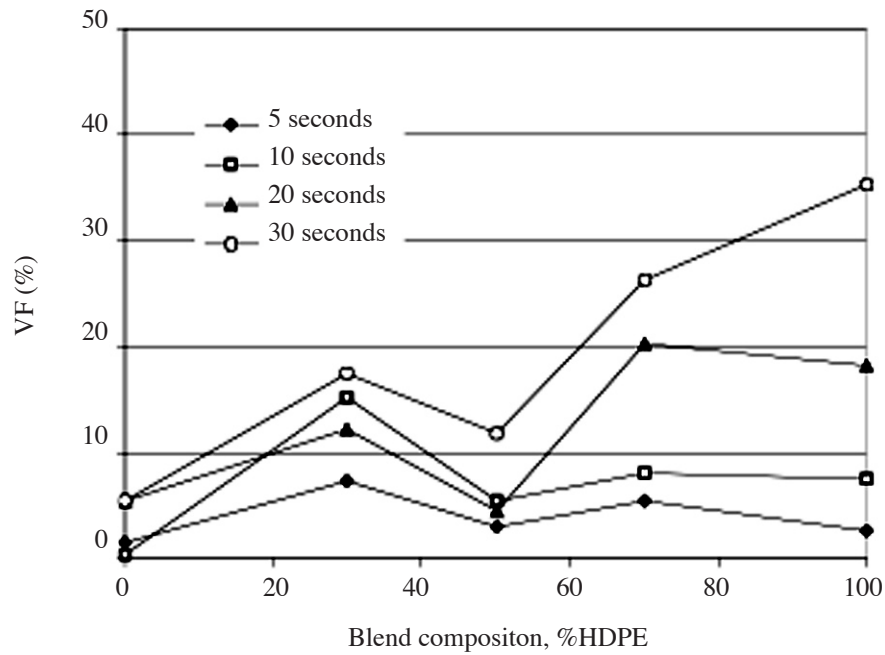


Figure 10. Effect of foaming time and blend composition on the void fraction at 160°C.

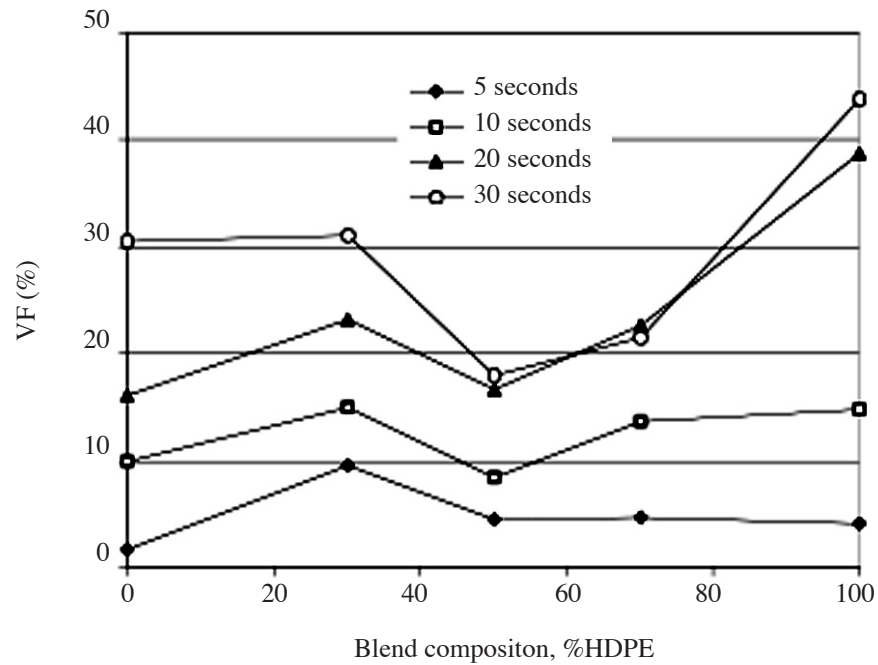


Figure 11. Effect of foaming time and blend composition on the void fraction at 175°C.

The blend of 50:50 HDPE/PP behaved strangely. The void fraction was lower than the other blends at all foaming times and temperatures. Moreover, the void fraction was even lower than that for HDPE and PP. For example, the void fraction of HDPE was above 40% and PP was around 30% for a foaming time of 30 seconds at 175°C, but the blend of 50:50 HDPE/PP had a void fraction of less than 20%. This is surprising in view of the results of

Doroudiani et al., (1998) who achieved the highest void fraction at this composition. The behavior of 50:50 HDPE/PP should be investigated further.

CONCLUSION

Solubility of CO₂ is dependent on the total amount of crystallinity in the polymers. Polymer blending decreased the crystallinity of HDPE and PP. Crystallinity of HDPE decreased dramatically as the PP component increased while crystallinity of PP slightly decreased as the HDPE component increased. To achieve a high-void fraction in these polyolefins required a foaming time of at least 20 seconds and a foaming temperature significantly above the melting temperature. The blend ratio also affected the ability to achieve a high-void fraction.

REFERENCES

- Baldwin, D. F., N. P. Suh, and M. Shimbo. 1992. Gas dissolution and crystallization in microcellular thermoplastic polyesters. *Cellular Polymers* 38: 109–128.
- Collias, D. I., D. G. Baird, and R. J. M. Borggreve. 1994. Impact toughening of polycarbonate by microcellular foaming. *Polymer* 35 (18): 3978–3983.
- Colton, J. S. 1989. The nucleation of microcellular foams in semi-crystalline thermoplastics. *Mater. Manuf. Proc.* 4: 253–262.
- Doroudiani, S., C. B. Park, and M. T. Kortschot. 1996. Effect of crystallinity and morphology on the microcellular foam structure of semicrystalline polymers. *Polymer. Eng. Sci.* 36 (21): 2645–2662.
- Doroudiani, S., C. B. Park, and M. T. Kortschot. 1998. Processing and characterization of microcellular foamed high-density polyethylene/isotactic polypropylene blends. *Polymer. Eng. Sci.* 38 (7): 1205–1215.
- Geol, S. K., and E. J. Beckman. 1994. Generation of microcellular polymeric foams using supercritical carbon dioxide. I: Effect of pressure and temperature nucleation. *Polymer. Eng. Sci.* 34: 1137–1148.
- Kumar, V., and N. P. Suh. 1988. Structure of microcellular thermoplastic foam. *SPE ANTEC Tech. Papers.* 34: 715–178.
- Kumar, V., and J. E. Weller. 1991. Microcellular polycarbonate Part I: Experiments on bubble nucleation and growth. *SPE ANTEC Tech. Papers.* 37: 1401–1405.
- Kumar, V., and M. M. Vander Wel. 1991. Microcellular polycarbonate Part II: Characterization of tensile modulus. *SPE ANTEC Tech. Papers.* 37: 1406–1410.
- Kumar, V., J. E. Weller, and R. Montecillo. 1992. Microcellular PVC. *SPE ANTEC Tech. Papers.* 38: 1452–1456.
- Kweeder, J. A., N. S. Ramesh, G. A. Campbell, and D.H. Rasmussen. 1991. Nucleation of microcellular polystyrene foam. *SPE ANTEC Tech. Papers.* 37: 1398–1400.
- Martini, J., F. A. Waldman, and N. P. Suh. U.S. Patent 4,473,665 (1984).
- Martuscelli, E. 1984. Influence of composition, crystallization conditions and melt phase structure on solid morphology, kinetics of crystallization and thermal behavior of binary polymer/polymer blends. *Polym. Eng. Sci.* 24: 563–586.

- Matuana, L. M., C. B. Park, and J. J. Balatinecz. 1996. Characterization of microcellular PVC/cellulosic-fibre composites. *J. Cellular Plast.* 32 (5): 449–467.
- Matuana, L. M., C. B. Park, and J. J. Balatinecz. 1997. Processing and cell morphology relationships for microcellular foamed PVC/cellulosic-fiber composites. *Polym. Eng. Sci.* 37 (7): 1137–1147.
- Matuana, L. M., C. B. Park, and J. J. Balatinecz. 1998(a). Cell morphology and property relationships of microcellular foamed PVC/wood-fiber composites. *Polym. Eng. Sci.* 38 (11): 1862–1872.
- Matuana, L. M., C. B. Park, and J. J. Balatinecz. 1998(b). Structures and mechanical properties of microcellular foamed polyvinyl chloride. *Cellular Polym.* 17 (1): 1–16.
- Matuana, L. M., and F. Mengeloglu. 2001. Microcellular foaming of impact-modified rigid PVC/wood-flour composites. *Journal of Vinyl and Additive Technology* 7 (2): 67–75.
- Seeler, K. A., and V. Kumar. 1993. Tension-tension fatigue of microcellular polycarbonate: initial results. *J. Reinforced Plast. Comp.* 12: 359–376.
- Seeler, K. A., and V. Kumar. 1994. Effect of CO₂ saturation and desorption on the notch sensitivity of polycarbonate fatigue. *SPE ANTEC Tech. Papers.* 40: 1972–1976.
- Shimbo, M., D. F. Baldwin, and N. P. Suh. 1992. Viscoelastic behavior of microcellular plastics. *Proc. of Polymeric Materials: Science and Engineering.* Amer. Chem. Soc. Conference. 67: 512–513.
- Wunderlich, B. 1973. *Macromolecular physics, Vol. 1, Crystal Structure, Morphology, Defects.* Academic Press, New York.

Page 32 none